A high order Spectral Volume method for moving boundary problems

R. Kannan[1]

CFD Research Corporation, Huntsville, Alabama, 35806

and

Z.J. Wang[2]

Department of Aerospace Engineering, Ames, Iowa, 50011

In this paper, we obtain inherently unsteady solutions to the Navier-Stokes equations involving moving boundaries. We employ a mapping function to map the grid and the flow features between a fixed reference frame and a moving reference frame. The actual equations of conservation (applicable on the moving reference frame) are then rewritten so as to form an altered set of equations, which are valid in the fixed reference frame. These altered set of equations are discretized and then solved using the high order spectral volume method (SV). The time advancement is carried out using the three stage Runge Kutta method. Simulations are performed to demonstrate the proof of the above concept and the ability of this method to handle more complicated motions.

Nomenclature

SV	=	spectral volume
CV	=	control volume
Q	=	vector of conserved variables
F_{inv}	=	inviscid flux vector
$\overline{Q}_{i,j}$	=	CV averaged conserved variable for C_{ij}
F_{vis}	=	viscous flux vectorpressure coefficient
N	=	Number of CVs in a SV
L(x,y)	=	Shape functions used for building a polynomial in a SV satisfy
$\vec{q}$	=	Auxilliary variable; is ∇u
$\underline{u}$, $\underline{\vec{q}}$	=	Numerical fluxes used for diffusion
R	=	Function mapping a fixed reference frame (X, Y, Z) to a moving reference frame (x, y, z)
J	=	Jacobian matrix : $\nabla_X R$
g	=	Determinant of J
w	=	Time derivative of R
$\hat{Q}$	=	Altered conserved variable
$\hat{F}_{inv}$	=	Altered inviscid flux vector
$\hat{F}_{vis}$	=	Altered viscous flux vector

---

[1] Research Engineer, CMB division, CFD Research Corporation, 215 Wynn drive, Huntsville, AL 35806.
[2] Professor of Aerospace Engg, Iowa state University, Associate editor AIAA.

1
American Institute of Aeronautics and Astronautics

I. Introduction

The spectral volume (SV) method was originally developed by Wang, Liu et al and their collaborators for hyperbolic conservation laws on unstructured grids. [22,23,24,25,26,14] The spectral volume method is a subset of the Godunov type finite volume method, which is the starting block for the development of a plethora of methods such as the k-exact finite volume[2,7], MUSCL[20,21], and the essentially non-oscillatory (ENO)[1,8] methods. The spectral volume method can be viewed as an extension of the Godunov method to higher order by adding more degrees-of-freedom (DOFs) in the form of subcells in each cell (simplex). The simplex is referred to as a spectral volume (SV) and the subcells are referred to as control volumes (CV). Every simplex in the SV method utilizes a "structured" pattern to construct the subcells (CVs). As in the finite volume method, the unknowns (or DOFs) are the subcell-averaged solutions. A finite volume procedure is employed to update the DOFs. The spectral volume method shares many simular properties with the discontinuous Galerkin (DG)[3,4] and the spectral difference (SD)[13,17] methods, such as discontinuous solution space and compactness. They mainly differ on how the DOFs are chosen and updated. Since the DG is a derivative of the finite element method, most implementations use the elemental nodal values as DOF, though some researchers use the equally valid modal approaches. Although both of the above approaches are mathematically identical, at least for linear equations, different choices of DOFs are used by various researchers result in different efficiency and numerical properties. The spectral volume being a derivative of the finite volume has subcell averages as its DOF while the spectral difference has point wise values as DOF. In terms of complexity, DG requires both volume and surface integrations. In contrast, SV requires only surface integrations and the SD requires differentiations.

The SV method was successfully implemented for 2D Euler[25] and 3D Maxwell equations[14]. Recently Sun et al[18] implemented the SV method for the Navier Stokes equations using the LDG[6] approach to discretize the viscous fluxes. Kannan and Wang[12] conducted some Fourier analysis for a variety of viscous flux formulations. An implicit LU-SGS algorithm was implemented in conjunction with a p-multigrid algorithm[12]. Even more recently, Kannan[10] extended the spectral volume formulation to solve the moment model equations in semiconductor device simulations.

In this paper, we extend the SV method to tackle moving boundary problems. Most of the real life applications involve time varying geometries. Examples of the above involve rotor-stator applications, thrust production in birds by flapping of wings and cases involving fluid-structure interaction. The high order DG method has been used in the past to accurately account for the time variation of the solution domain[15]. The Geometric Conservation Law (GCL) was used to ensure the preservation of constant flow solutions, under arbitrary grid deformations. However for some simple motions (including pure translations and some rotations), the GCL is automatically satisfied. This paper focuses on such types of moving problems.

In this paper, we follow a similar approach to that presented using the above DG formulations[15,9]. The spatial discretization is carried out using the SV method on a mesh of triangles, and the time integration is done with an explicit multi-stage strong stability preserving Runge–Kutta scheme. The equations are discretized on a fixed reference frame. A continuous function maps this fixed reference frame to a moving reference frame. The Jacobian matrix of the above transformation is given by $J = \nabla_X R$ and the determinant of this Jacobian matrix is g. As mentioned earlier, we restrict our simulations to those problems, wherein GCL is automatically satisfied. This eliminates the need to solve an additional scalar equation (for time evolution of g).

The paper is, therefore, arranged in the following manner. In the next section, we review the basics of the SV method. The fundamentals of extending the SV to moving grids are presented in section 3. Section 4 presents with the two test cases conducted in this study. Finally conclusions from this study are summarized in Section 5.

II. Basics of the spectral volume method

Consider the general conservation equation:

$$\frac{\partial Q}{\partial t} + \nabla \cdot (F_{inv}(Q) - F_{vis}(Q, \nabla Q)) = 0, \tag{2.1}$$

in domain Ω with appropriate initial and boundary conditions . In (2.1), Q is the vector of conserved variables, and F_{inv} and F_{vis} are the inviscid and viscous flux vectors. Domain Ω is discretized into I non-overlapping triangular (2D) cells. In the SV method, the simplex grid cells are called SVs, denoted S_i, which are further partitioned into CVs, denoted C_{ij}, which depend on the degree of the polynomial reconstruction. Figure 1 shows linear, quadratic and cubic partitions in 2D.
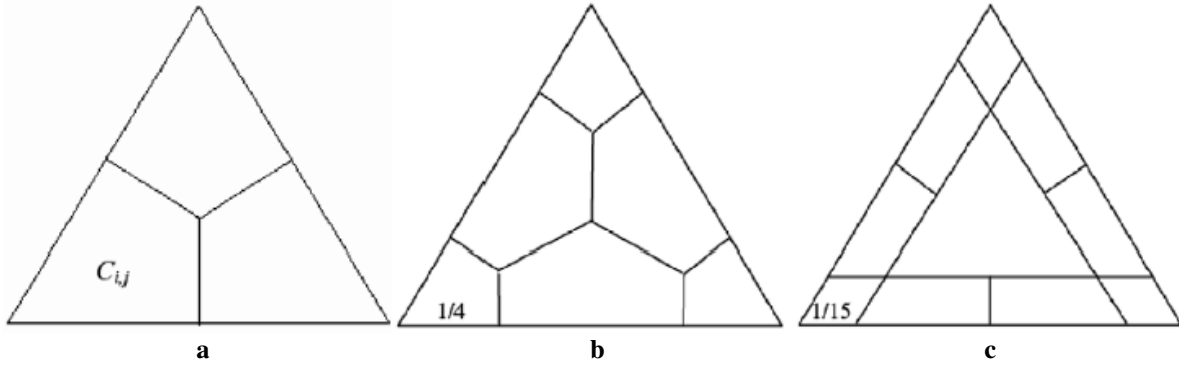
Figure 1.Partitions of a triangular SV . Linear, quadratic and cubic reconstructions are shown in a, b and c respectively.

We need N unknown control volume solution averages (or DOFs) to construct a degree k polynomial. N is calculated using the below formula (in 2D)

$$N = \frac{(k+1)(k+2)}{2}, \tag{2.2}$$

where k is the degrees of the polynomial, constructed using the CV solution averages. The CV averaged conserved variable for C_{ij} is defined as

$$\overline{Q}_{i,j} = \frac{1}{V_{i,j}} \int_{C_{i,j}} Q dV , \text{ j=1...N, i=1...I}, \tag{2.3}$$

where $V_{i,j}$ is the volume of C_{ij}. Given the CV averaged conserved variables, a degree k polynomial can be constructed such that it is $(k+1)^{th}$ order approximation to Q. In other words, we can write the polynomial as

$$p_i(x, y) = \sum_{j=1}^{N} L_j(x, y)\overline{Q}_{i,j} , \tag{2.4}$$

where the shape functions $L_j(x,y)$ satisfy

$$\frac{1}{V_{i,j}} \int_{C_{i,j}} L_n(x, y) dV = \delta_{j,n}. \tag{2.5}$$

Equation 2.1 is integrated over the C_{ij}. This results in the following equation

$$\frac{\partial \overline{Q}}{\partial t} + \frac{1}{V_{i,j}} \sum_{r=1}^{K} \int_{Ar} (\vec{F}.\vec{n}) dA = 0, \tag{2.6}$$

where $\vec{F} = (f_i - f_v, g_i - g_v)$ where A_r represents the rth face of C_{ij}, $\vec{n}$ is the outward unit normal vector of A_r and K is the number of faces in C_{ij}. The surface integration on each face is done using a $(k+1)^{th}$ order accurate Gauss quadrature formula. The fluxes are discontinuous across the SV interfaces. The inviscid fluxes are handled using a numerical Riemann flux such as the Rusanov flux, the Roe flux or AUSM flux. The handling of the viscous fluxes is discussed in the next section.

A. Spectral volume formulation for the diffusion equation

The following 2D diffusion equation is considered first in domain Ω with appropriate initial and boundary conditions

$$\frac{\partial u}{\partial t} - \nabla \cdot (\mu \nabla u) = 0, \tag{2.7}$$

where μ is a positive diffusion coefficient. We define an auxiliary variable

$$\vec{q} = \nabla u. \tag{2.8}$$

Equation 2.7 then becomes

$$\frac{\partial u}{\partial t} - \nabla \cdot (\mu \vec{q}) = 0. \tag{2.9}$$

Using the Gauss-divergence theorem, we obtain

$$\overline{\vec{q}}_{ij} V_{ij} = \sum_{r=1}^{K} \int_{Ar} u \cdot \vec{n} dA, \tag{2.10}$$

$$\frac{d\overline{u}_{ij}}{dt} V_{ij} - \sum_{r=1}^{K} \int_{A_r} \mu \vec{q} \cdot \vec{n} dA = 0, \tag{2.11}$$

where $\overline{\vec{q}}_{ij}$ and $\overline{u}_{ij}$ are the CV averaged gradient and solution in C_{ij}. As the solution u is cell-wise continuous, u and $\vec{q}$ at SV boundaries are replaced by numerical fluxes $\underline{\vec{q}}$ and $\underline{u}$. The above equations thus become

$$\overline{\vec{q}}_{ij} V_{ij} = \sum_{r=1}^{K} \int_{Ar} \underline{u} \cdot \vec{n} dA, \tag{2.12}$$

$$\frac{d\overline{u}_{ij}}{dt} V_{ij} - \sum_{r=1}^{K} \int \mu \underline{\vec{q}} \cdot \vec{n} dA = 0. \tag{2.13}$$

The commonly used approach for obtaining the numerical fluxes is the LDG approach. This procedure was developed by Cockburn and Shu[5,6]. This method dealt with rewriting a second-order equation as a first-order system and then discretize the first-order system using the DG formulation. Their simplicity and effectiveness have made them the main choice for discretizing the viscous fluxes. In this approach, the numerical fluxes are defined by alternating the direction in the following manner[18]

$$\underline{u} = u_L, \tag{2.14}$$

$$\underline{\vec{q}} = \vec{q}_R, \tag{2.15}$$

where u_L and u_R are the left and right state solutions of the CV face in consideration and $\vec{q}_L$ and $\vec{q}_R$ are the left and right state solution gradients of the face (of the CV) in consideration. Thus if the CV face lies on the SV boundary, $u_L \neq u_R$ and $\vec{q}_L \neq \vec{q}_R$.

All the simulations performed during the course of this study employed the LDG formulation for discretizing the viscous flux.

III. Extending SV to moving grids

Persson et al[15] was one of the first few researchers to use an Arbitrary lagrangian-Eulerian (ALE) formulation for high order simulations. A discontinuous Galerkin (DG) formulation was used by the above researchers. More recently Jameson et al[9] used the ALE formulation to perform simulations of unsteady flow past a plunging airfoil using a high order spectral difference (SD) method.

A. The transformation

Let R denote a continuous function which maps a fixed reference frame (X, Y, Z) to a moving reference frame (x, y, z) ; thus in other words, $(x, y, z) = R(X, Y, Z, t)$. The Jacobian matrix of the above transformation is given by $J = \nabla_X R$ and the determinant of this Jacobian matrix is g. The mapping velocity w is the time derivative of the transformation R. This is the velocity with which the body moves (can be translation, rotation or deformation) in space.

B. The altered equations

The equations of conservation (valid in the moving reference frame) can be rewritten so as to enable equally mathematically valid altered conservation equations in the fixed reference frame. The altered equations can be written in the following manner:

$$\frac{\partial \hat{Q}}{\partial t} + \nabla \cdot (\hat{F}_{inv}(\hat{Q}) - \hat{F}_{vis}(\hat{Q}, \nabla \hat{Q})) = 0 , \tag{3.1}$$

where $\hat{Q} = gQ$, $\hat{F}_{inv} = gJ^{-1}F_{inv} - \hat{Q}J^{-1}w$ and $\hat{F}_{vis} = gJ^{-1}F_{vis}$.

C. Geometric conservation law

The conservation of a constant flow is a necessary condition for any viable numerical scheme. Otherwise mass, momentum or energy would be produced unphysically by the numerical simulation. A constant solution should be preserved inspite of all the extra terms created by the grid motion. This is the so-called Geometric Conservative Law.

Persson et al[15] showed that for arbitrary mappings, a constant solution in the physical domain is not necessarily a solution of the discretized equations in the fixed reference frame. They were able to pin point the creation of the associated error in the integration step of the determinant g. The following equation represents the time advancement of the determinant g :

$$\frac{\partial g}{\partial t} + \nabla \cdot (gJ^{-1}w) = 0, \tag{3.2}$$

For trivial cases (like pure translations, rotations), the above equation is automatically satisfied. For more complicated cases, the above equation needs to be integrated using a numerical scheme. More details on the above can be found in Persson et al[15].

D. Special case scenario

As mentioned earlier, for some cases, equation 3.2 is automatically satisfied. More specifically for pure translation based motions, the Jacobian matrix $J = [I]$. This implies that $g = 1$. The altered equations can be written in the following manner:

$$\frac{\partial Q}{\partial t} + \nabla \cdot (\hat{F}_{inv}(Q) - F_{vis}(Q, \nabla Q)) = 0, \tag{3.3}$$

where $\hat{F}_{inv} = F_{inv} - Qw$.

The inviscid numerical flux is obtained using the Rusanov formulation i.e.

$$\tilde{\tilde{F}}_{inv} = \frac{(\hat{F}_{inv}(Q_L) + \hat{F}_{inv}(Q_R))}{2} - \alpha \frac{(Q_R - Q_L)}{2}, \tag{3.4}$$

where $\tilde{\tilde{F}}_{inv}$ is the numerical inviscid flux, $\alpha = \max |\frac{\partial \hat{F}_{inv}(Q)}{\partial Q}| = c + abs((\vec{v} - \vec{w}).\vec{n})$, c is the sound speed and $\vec{v}$ is the velocity vector.

The LDG formulation is used to discretize the viscous flux.

IV. Time integration algorithms

All the simulations performed in this paper use a three stage SSP SSP Runge kutta scheme. The three-stage explicit SSP Runge Kutta[16] can be written as follows:

$$\bar{u}_i^{(1)} = \bar{u}_i^n - \Delta t R_i(\bar{u}^n);$$

$$\bar{u}_i^{(2)} = \frac{3}{4}\bar{u}_i^n + \frac{1}{4}[\bar{u}_i^{(1)} - \Delta t R_i(\bar{u}^{(1)})];$$

$$\bar{u}_i^{n+1} = \frac{1}{3}\bar{u}_i^n + \frac{2}{3}[\bar{u}_i^{(2)} - \Delta t R_i(\bar{u}^{(2)})]. \tag{4.1}$$

V. Test results

In this Section, the recently adapted SV method is tested for some moving boundary flow problems. The following two cases are presented.

A. Flow over a moving airfoil

This case was selected to validate the moving grid SV solver. An airfoil moves from right to left in quiescent air with a Mach number of 0.6. If the reference frame is fixed on the moving airfoil, the flow field should reach a steady state after the initial transients propagate out of the solution domain. The computational grid (SV grid) is shown in figure 2.

American Institute of Aeronautics and Astronautics
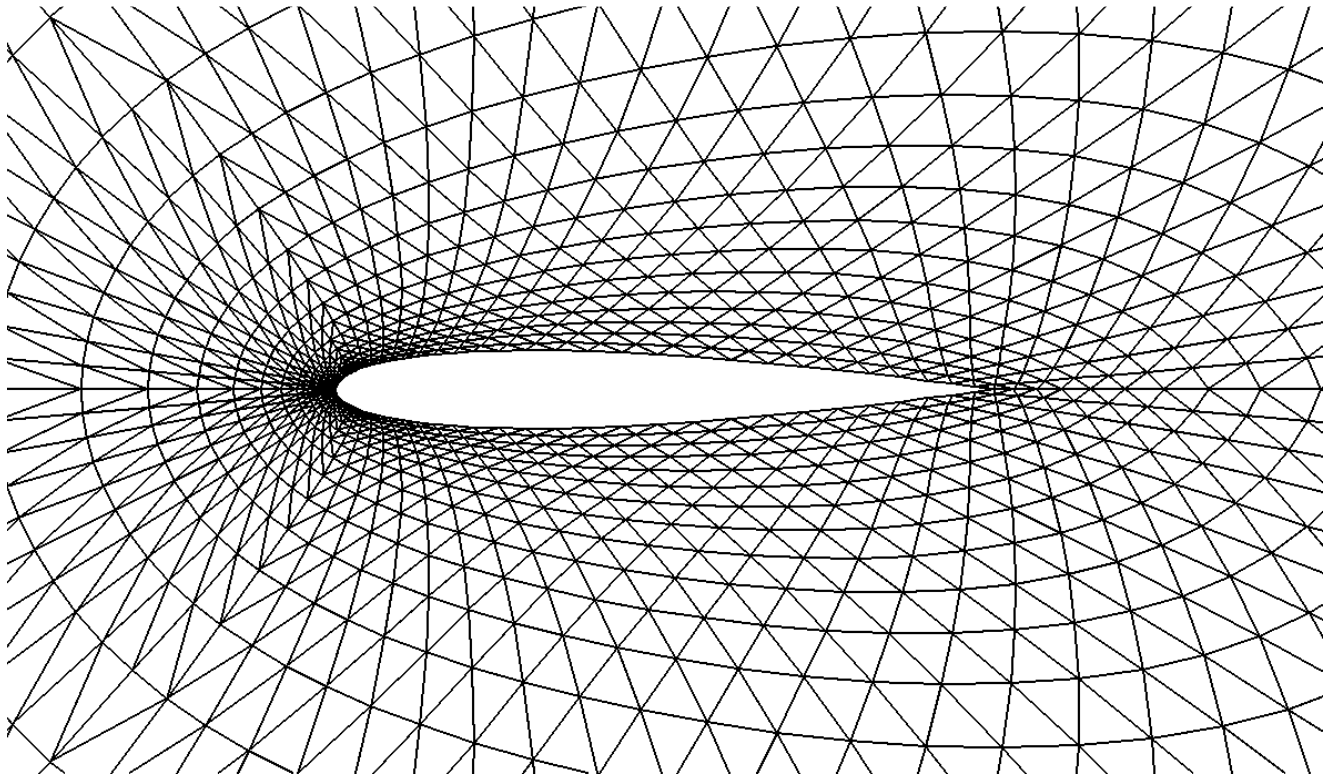
Figure 2. SV Grid (72*24*2) used for the subsonic flow over the NACA 0012

A.1 Inviscid flow over a moving airfoil

The outer boundary of the computational grid is located 20 times the chord length away from the centroid of the airfoil. The pressure distributions at two different times are displayed in Figures 3 and 4. Note that initially a very high/low pressure region was created on the left/right side of the airfoil due to the sudden motion. As time goes, the flow field becomes nearly "steady" for an observer stationed on the airfoil. In fact, the pressure field created by the moving airfoil after a long time is compared with that created by a free stream of Mach 0.6 over a stationary airfoil in Figure 3 and 4. It is observed that the pressure fields are very similar.

American Institute of Aeronautics and Astronautics
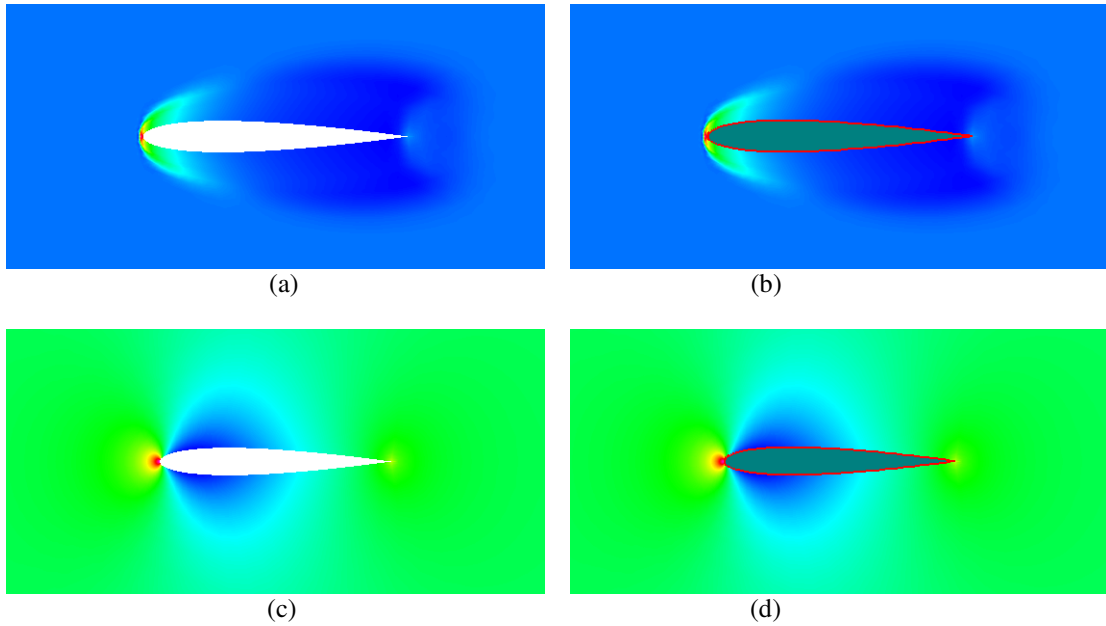
Figure 3. Inviscid pressure distribution obtained by second order simulations. Case (a): Initial transient obtained for flow over a stationary airfoil; Case (b): Initial transient obtained by using the moving body method. Case (c): Steady state pressure obtained for flow over a stationary airfoil; Case (d): Steady state pressure obtained by the moving body method.
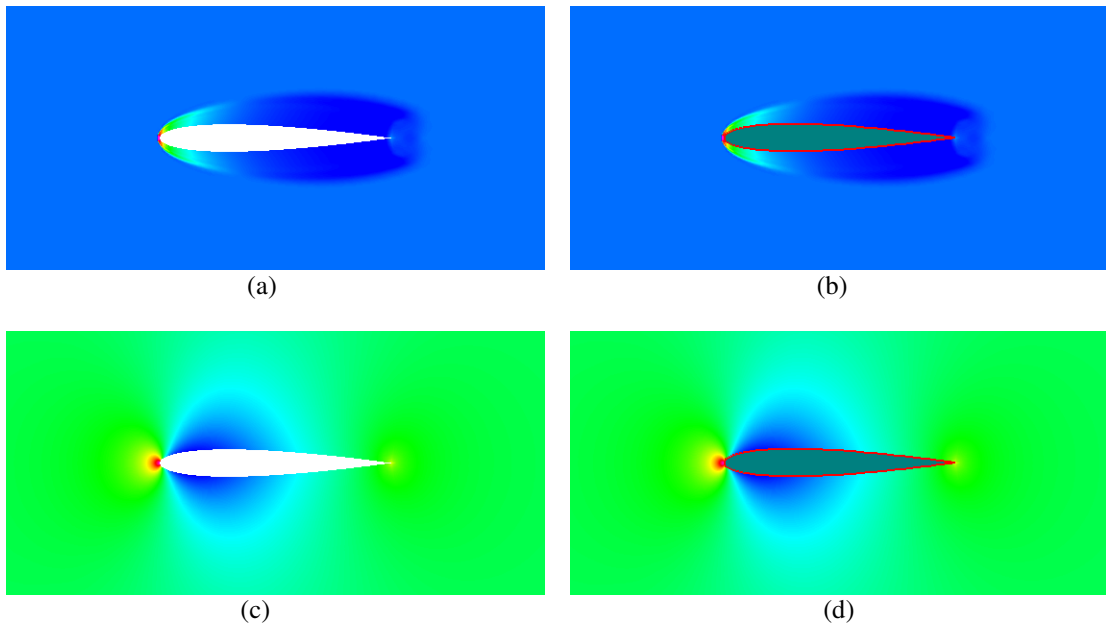
Figure 4. Inviscid pressure distribution obtained by third order simulations. Case (a): Initial transient obtained for flow over a stationary airfoil; Case (b): Initial transient obtained by using the moving body method. Case (c): Steady state pressure obtained for flow over a stationary airfoil; Case (d): Steady state pressure obtained by the moving body method.

American Institute of Aeronautics and Astronautics

A.2 Laminar flow over a moving airfoil

For this simulation, the airfoil was moved from the right to the left in quiescent air. The fluid was assumed to be laminar. The Reynolds number was 1000. As time goes, the flow field becomes nearly "steady" for an observer stationed on the airfoil. This is seen in Figure 5. In general, the match between the moving case and the stationary case was very good.

(a)   (b)

(c)   (d)
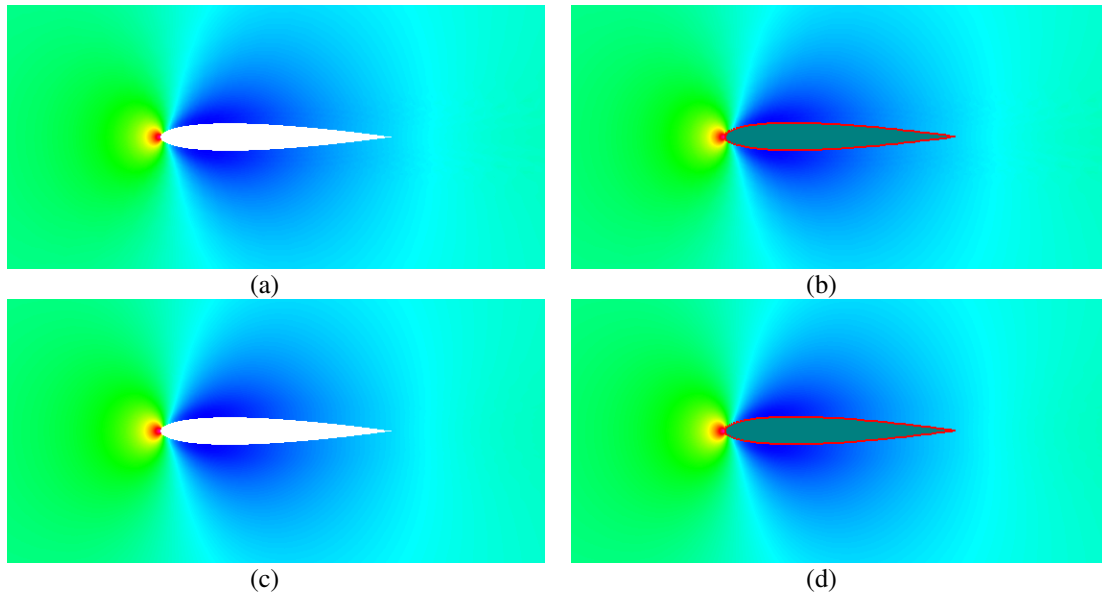
Figure 5. Laminar pressure distribution over an airfoil. Case (a): Steady state pressure obtained for flow over a stationary airfoil using second order simulations ; Case (b): Steady state pressure obtained by the moving body method using second order simulations; Case (c): Steady state pressure obtained for flow over a stationary airfoil using third order simulations ; Case (d): Steady state pressure obtained by the moving body method using third order simulations.

B. The plunging airfoil problem

We consider the plunging airfoil problem test problem. This has been a standard test case for moving body simulations[11,15,9]. The airfoil in consideration is a NACA-0012 airfoil. It is exposed to an incoming flow at Mach 0.2 and the Reynolds number based on the incoming flow velocity is 1850. The airfoil plunges according to the prescribed formula: $Y = h * \sin(wt)$. A value of 1.15 for w and 0.08c for h was used. This corresponds to a Strouhal number of 0.46.

Figure 6 shows the coefficient of drag (from pressure) obtained using the 2nd and the 3rd order formulations. It can be seen that the above is periodic and a time averaging of the drag coefficient results in a negative number. It is observed that the airfoil generates thrust and not drag. Vortices shed by the airfoil during the first downstroke and upstroke motions are shown in figures 7 and 8 respectively. It can be seen that the 2nd order simulations cause much higher dissipation of the shed vortices than the 3rd order simulations. This alignment of the vortices results in a positive x component of velocity (behind the airfoil). This corresponds to a thrust indicative pattern as explained by Von Karman[19].
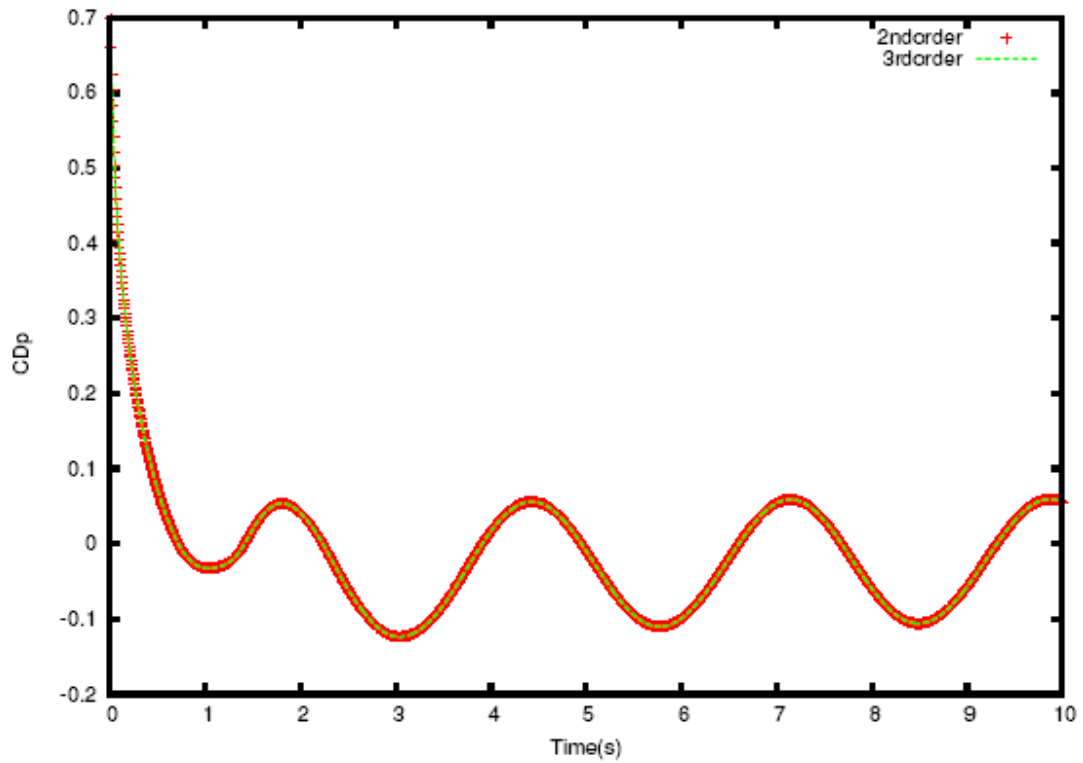
Figure 6. Coefficient of drag due to pressure for the heaving airfoil (Strouhal number = 0.46).

a

b
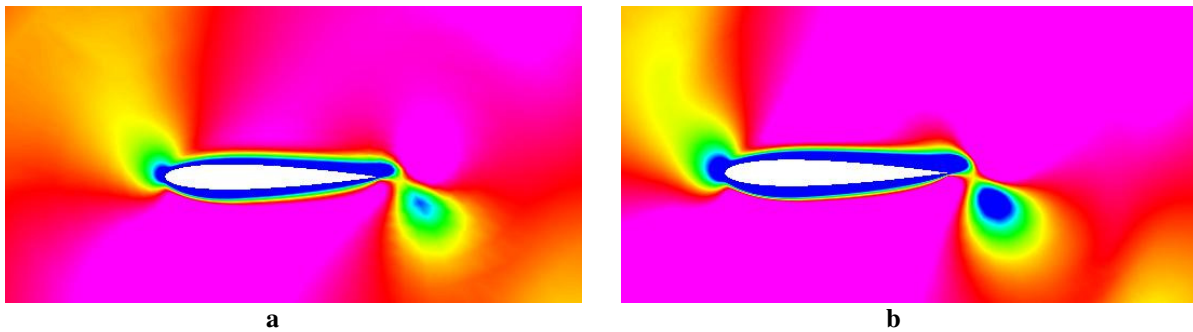
Figure 7. Vortex shed by the airfoil during the first downstroke motion. Case (a): 2nd order simulation; Case (b): 3rd order simulation.

a

b
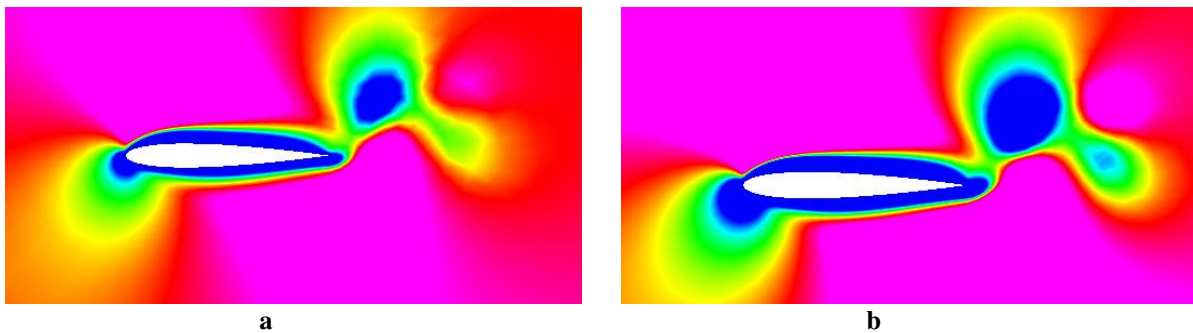
Figure 8. Vortex shed by the airfoil during the first upstroke motion. Case (a): 2nd order simulation; Case (b): 3rd order simulation.

American Institute of Aeronautics and Astronautics

Two other simulations, with progressively larger heaving frequencies were attempted: corresponding to Strouhal numbers of 0.628 and 0.942. The coefficient of drag due to pressure for the above cases is shown in figures 9 and 10. It can be inferred that an increase in Strouhal number increases the amount of thrust produced.
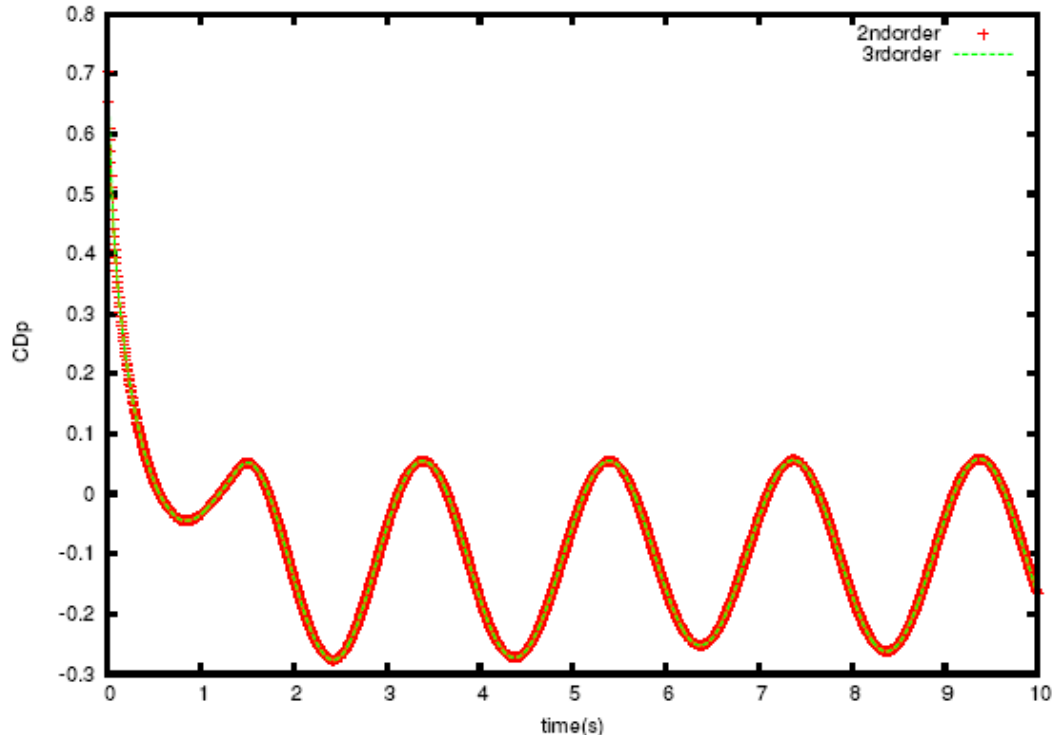
Figure 9. Coefficient of drag due to pressure for the heaving airfoil (Strouhal number = 0.628).
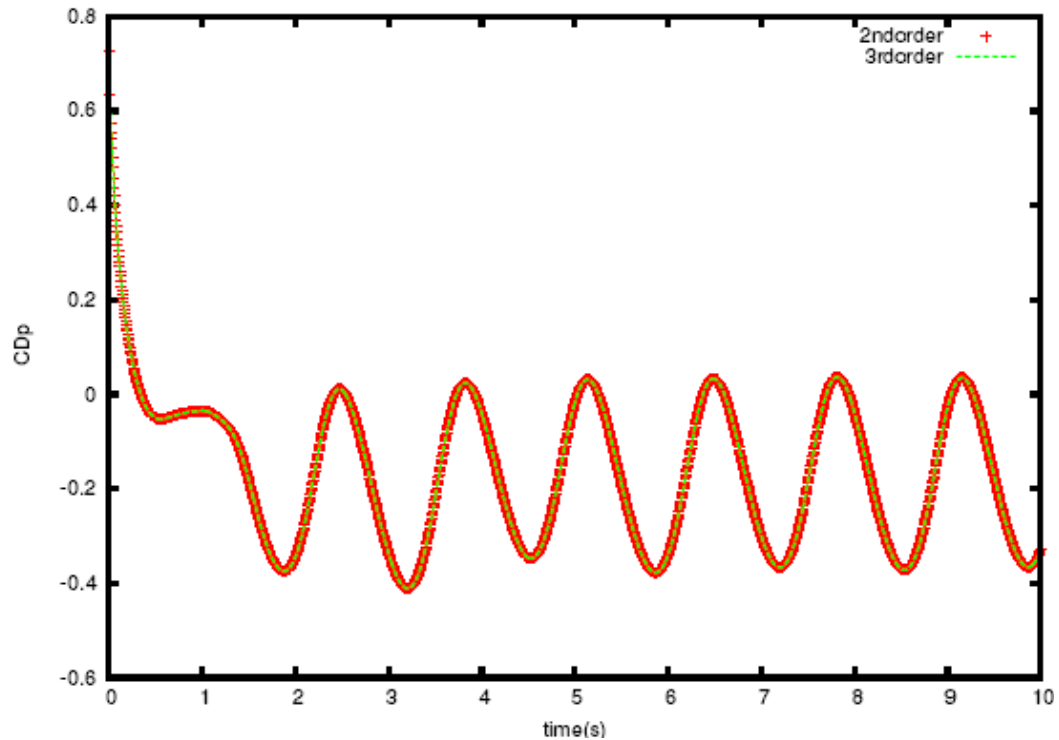
Figure 10. Coefficient of drag due to pressure for the heaving airfoil (Strouhal number = 0.942).

11
American Institute of Aeronautics and Astronautics

VI. Conclusions

In this paper, we extended the SV method to tackle some basic moving boundary problems. The spatial discretization is carried out using the SV method on a mesh of triangles, and the time integration is done with an explicit multi-stage strong stability preserving Runge–Kutta scheme. The equations are discretized on a fixed reference frame. A continuous function maps this fixed reference frame to a moving reference frame. As mentioned earlier, we restrict our simulations to those problems, wherein GCL is automatically satisfied.

The flow over an airfoil was simulated to validate the moving grid SV solver. The pressure field created by the moving airfoil was compared with that created by a free stream of Mach 0.6 over a stationary airfoil. The pressure fields were identical.

The moving grid SV solver was used to solve the plunging airfoil problem test problem. The airfoil was exposed to an incoming flow at Mach 0.2 and the Reynolds number based on the incoming flow velocity was 1850. The airfoil plunges according to the prescribed formula: $Y = h * \sin(wt)$. Vortices shed by the airfoil during the first downstroke and upstroke motions were captured. The 2nd order simulations caused much higher dissipation of the shed vortices than the 3rd order simulations. This alignment of the vortices resulted in a positive x component of velocity (behind the airfoil). This corresponds to a thrust indicative pattern as explained by Von Karman[19].

Future work would involve high-order accurate simulations of laminar flow past flapping wing micro air vehicles (MAVs) with more complex motions.

References

[1] R. Abgrall, "On essentially non-oscillatory schemes on unstructured meshes: analysis and implementation", J. Comput. Phys. 114 (1994) 45–58.

[2] T.J. Barth and P.O. Frederickson, "High-order solution of the Euler equations on unstructured grids using quadratic reconstruction", AIAA Paper No. 90-0013, 1990.

[3] F. Bassi and S. Rebay.,"GMRES discontinuous Galerkin solution of the compressible Navier-Stokes equations", In Karniadakis Cockburn and Shu, editors, Discontinuous Galerkin Methods: Theory, Computation and Applications, pages 197–208. Springer, Berlin, 2000.

[4] F. Bassi and S. Rebay, "Numerical solution of the Euler equations with a multiorder discontinuous Finite element method", in: Proceedings of the Second International Conference on Computational Fluid Dynamics, Sydney, Australia, 15–19 July 2002.

[5] B. Cockburn and C. W. Shu., "Runge-Kutta discontinuous Galerkin methods for convection-dominated problems", J. of Sci. Comput., 16(3):173–261, September 2001.

[6] B. Cockburn and C.-W. Shu, "The local discontinuous Galerkin method for time-dependent convection diffusion system", SIAM J. Numer. Anal. 35 (1998) 2440–2463.

[7] M. Delanaye and Yen Liu, "Quadratic reconstruction finite volume schemes on 3D arbitrary unstructured polyhedral grids", AIAA Paper No. 99-3259-CP, 1999.

[8] A. Harten, B. Engquist, S. Osher and S. Chakravarthy, "Uniformly high order essentially non-oscillatory schemes III", J. Comput. Phys. 71 (1987) 231.

[9] A. Jameson and C. Liang, "Unsteady flow past a plunging airfoil", Workshop on Vortex Dominated Flows, June, 2009, National Institute of Aerospace.

[10] R. Kannan, "An Implicit LU-SGS Spectral Volume Method for the Moment Models in Device Simulations: Formulation in 1D and application to a p-multigrid algorithm", International Journal for Numerical Methods in Biomedical Engineering (formerly Communications in numerical methods in engineering), accepted on October 11, 2009, Published Online: 1 Feb 2010

[11] R. Kannan and Z.J. Wang, "A Parallel Overset Adaptive Cartesian/Prism Grid Method for Moving Boundary Flows", International conference on CFD, 2006, Ghent, Belgium.

[12] R. Kannan and Z.J. Wang, "A study of viscous flux formulations for a p-multigrid spectral volume Navier stokes solver", Journal of Scientific Computing, <u>Volume 41, Number 2, November, 2009</u>.

[13]C. Liang, R. Kannan and Z.J. Wang, "A-p-multigrid Spectral Difference method with explicit and implicit smoothers on unstructured grids", Computers & Fluids, Volume 38, Issue 2, February 2009, Pages 254-265.

[14]Y. Liu, M. Vinokur and Z.J. Wang, "Spectral (finite) volume method for conservation laws on unstructured grids V: extension to three-dimensional systems", J Comput Phys 2006; 212:454–72.

[15]P.O. Persson, J. Bonet and J. Peraire," Discontinuous Galerkin solution of the Navier–Stokes equations on deformable domains", Comput. Methods Appl. Mech. Engg. 198 (2009) 1585–1595.

[16]Shu C-W. Total-variation-diminishing time discretizations. SIAM J Sci Stat Comput 1988;9:1073–84. Navier–Stokes equations on triangular meshes. AIAA J

[17]Y. Sun and Z.J. Wang,"Efficient Implicit Non-linear LU-SGS Approach for Compressible Flow Computation Using High-Order Spectral Difference Method", Communications in Comput. Phys (submitted)

[18]Y. Sun, Z.J. Wang and Y. Liu, "Spectral (finite) volume method for conservation laws on unstructured grids VI: Extension to viscous flow", J. Comput. Phys.2006; 215:41-58.

[19]T. Von Karman and J.M. Burgers, "General Aerodynamic Theory-Perfect Fluids," Aerodynamic Theory, Vol. 2. Julius-Springer, Berlin, 1943, p. 308.

[20]B. Van Leer, "Towards the ultimate conservative difference scheme II. Monotonicity and conservation combined in a second order scheme", J. Comput. Phys. 14 (1974) 361.

[21]B. Van Leer, "Towards the ultimate conservative difference scheme V. A second order sequel to Godunov's method", J. Comput. Phys. 32 (1979) 101.

[22]Z.J. Wang, "Spectral (finite) volume method for conservation laws on unstructured grids: basic formulation", J. Comput. Phys. 178 (2002) 210.

[23]Z.J. Wang and Y. Liu, "Spectral (finite) volume method for conservation laws on unstructured grids II: extension to two-dimensional scalar equation", J. Comput. Phys. 179 (2002) 665.

[24]Z.J. Wang and Y. Liu, "Spectral (finite) volume method for conservation laws on unstructured grids III: extension to one-dimensional systems", J. Sci. Comput. 20 (2004) 137.

[25]Z.J. Wang and Y. Liu, "Spectral (finite) volume method for conservation laws on unstructured grids IV: extension to two-dimensional Euler equations", J. Comput. Phys. 194 (2004) 716.

[26]Z.J. Wang and Y. Liu, "Extension of the spectral volume method to high-order boundary representation", J. Comput. Phys. 211 (2006) 154–178.